

Article

Pleistocene Glaciations of the Northwest of Iberia: Glacial Maximum Extent, Ice Thickness, and ELA of the Soajo Mountain

Edgar Figueira ^{1,*}, Alberto Gomes ^{1,2,*}  and Augusto Pérez-Alberti ³ ¹ Department of Geography, University of Porto, 4150-564 Porto, Portugal² CEGOT—Centre of Studies in Geography and Spatial Planning, Faculty of Arts and Humanities of Porto, University of Porto, 4150-564 Porto, Portugal³ Department of Soil Science and Agricultural Chemistry, Faculty of Biology, Campus Vida, University of Santiago de Compostela, 15782 Santiago de Compostela, Spain; augusto.perez@usc.es

* Correspondence: up201604568@edu.letras.up.pt (E.F.); atgomes@letras.up.pt (A.G.)

Abstract: Soajo Mountain is located in the northwestern Iberian Peninsula near the border between Portugal and Spain. Its highest elevation is 1416 m at the Pedrada summit. During the Pleistocene, the cascade cirques on the east flank and the icefield that covered the flattened surface of the high plateau generated several glacier valleys. This study presents a paleoglacial reconstruction of the relict glacial landscape in Soajo Mountain for the Glacial Maximum Extent (GME) through the following methods: (1) a detailed geomorphological map supported by high-resolution orthophotography, digital elevation models with a spatial resolution of 70 cm, and field surveys; (2) the delineation of the glacial surface, and the calculation of the glacial flowlines to obtain the numerical model of the ice thickness; and (3) an estimation of the paleoELA altitudes. The paleoglacial reconstruction, using GlaRe methodology, reveals a glacial surface of 16 km², including an icefield on the Lamas de Vez plateau (mean elevation of 1150 m) and a radial glacial flow to the east and north. The arrangement of the glaciated area attests to the topographic, lithological, and structural conditioning on the development of small glacial tongues, with an emphasis on the ice tongue flowing northwards, with a thickness of 173 m and a length of 2.92 km. The Soajo GME paleoglacier comprises three main glacial sectors: Lamas de Vez Icefield, Vez and Aveleira Valleys, and the Eastern Glacial Sector. These paleoglaciers have achieved maximum ice volumes of 214.4 hm³, 269.2 hm³, and 115.8 hm³, respectively, with maximum ice thicknesses of 127 m, 173 m, and 118 m, respectively. On the west flank, a smaller paleoglacier named Branda da Gémea recorded an ice volume of 24.3 hm³ and a maximum ice thickness of 110 m. According to the ELA-AABR method, Soajo Mountain has one of the lowest ELA values in the Iberian NW, ranging from 1085 to 1057 m. This is due to its oceanic location, an orographic barrier effect, and the influence of the polar front.



Citation: Figueira, E.; Gomes, A.; Pérez-Alberti, A. Pleistocene Glaciations of the Northwest of Iberia: Glacial Maximum Extent, Ice Thickness, and ELA of the Soajo Mountain. *Land* **2023**, *12*, 1226. <https://doi.org/10.3390/land12061226>

Academic Editor: Enrique Serrano Cañadas

Received: 30 April 2023

Revised: 5 June 2023

Accepted: 9 June 2023

Published: 13 June 2023



Copyright: © 2023 by the authors. Licensee MDPI, Basel, Switzerland. This article is an open access article distributed under the terms and conditions of the Creative Commons Attribution (CC BY) license (<https://creativecommons.org/licenses/by/4.0/>).

Keywords: glacial reconstructions; GlaRe; ELA; Soajo Mountain; Portugal

1. Introduction

The understanding of the Quaternary climatic evolution of the Earth can be supported by the analysis of glacial landforms. The existence and geographic location of glacial landforms are excellent geomorphic markers to evaluate the landscape response to the glacial and interglacial stages [1].

Mountainous landscapes are archives of local past climates [2], since they can preserve glacial landforms that reflect the age and intensity of the specific cold conditions necessary for their genesis. The study of glaciers and glaciations in a mountainous context depends directly on prior knowledge of the location, typology, and processes inherent to each morphology [3,4]. In mountain paleoglacial environments, the advantage of the existence

of glacial deposits, especially moraine ridges and erratic blocks, is the possibility of defining possible limits corresponding to several glacial phases [5,6].

The reconstruction of paleoglacial dynamics is a key challenge to understanding the current landscape of ancient paleoglaciated mountain areas [7,8] and to analysing the variations of their local cold conditions during the Upper Pleistocene [6].

Therefore, the detailed geomorphological study of glacial landforms allows, subsequently, the reconstruction of the paleoglacial masses responsible for the evolution and current state of mountainous landscapes [9]. Currently, with a detailed geomorphological map and a good interpretation of the inherited glacial forms, by using several available modelling tools, such as the GlaRe and ELA calculation toolboxes [10,11] (Supplementary Materials), it is possible to obtain an accurate reconstruction of paleoglaciers, namely, by obtaining accurate areas of maximum extent, and values of ice thickness and ELA.

On the Iberian northwest massifs, it is common to find glacial landforms inherited from Pleistocene glaciations [12]. All these cold-related landforms can be used as paleoclimatic and geomorphological indicators in paleoglacial studies by reconstructing ancient glacial environments using qualitative and quantitative measurements [5,7,13–15] even though the glacial processes are now extinct in northwest Iberia.

These paleoglacial reconstructions enable comparisons between current glacier morphologies, with the aim of using active glaciers to explain and comprehend the behaviour of extinct glaciers. These comparisons can be made using data from office interpretation, field reconnaissance and validation, geomorphological mapping [11,16], and the obtaining of ages to establish a geochronology of the process [9].

The mountainous landscape of the northwestern Iberian ranges is marked by the existence of significant and low mountain paleoglaciers, including those in the Serra del Xistral, Faro de Avión, Peneda-Gerês massifs, Montes de Cebreiro, Serra de Ancares, Serra do Courel, Manzaneda massif, Serra del Teleno, and Trevinca massif [9,17,18]. For the Soajo mountain (1416 m a.s.l., and hereinafter referred to as Serra do Soajo) located in northern Portugal and part of the Peneda-Gerês mountain range, previous research was concerned with the identification and mapping of the glacial landforms and their climatic significance [19–31]. Coudé-Gaussen [19] conducted the most relevant study for the Serra do Soajo by (1) identifying and mapping glacial landforms; (2) delineating the plausible limits of the Glacial Maximum Extent (GME) based on glacial reconstructions and Equilibrium-Line Altitude (ELA) values; and (3) explaining and interpreting the factors that contributed to the occurrence and spatial configuration of the glaciated area. Supported by field data, Coudé-Gaussen et al. [20] proposed an approach for the regional permanent snow line of Minho between 1100 and 1000 m. Based on the Maximum Elevation of Lateral Moraines (MELM) for the Soajo-Peneda-Gerês massifs, Pérez-Alberti [23] established a general reconstruction of the glaciated area for the GME and set the lowest ELA value at 773 m.

Despite these recent advances in the understanding of the mountain's glaciation in northwest Portugal, a systematic inventory of glacial forms and deposits, as well as their thorough, detailed geomorphological mapping, is still lacking. This gap makes it difficult to correctly interpret the distribution of the glacial landforms, calculate the ice thickness and the ELA values, and discuss the significance of these inherited glacial areas on local and regional scales. Since LiDAR point clouds have been recently made available for the Serra do Soajo, topographic recognition and new understandings of the region's glacial landforms have become possible, allowing us to move beyond the geomorphological uncertainty of earlier studies.

The aim of this study was to perform a paleoglacial reconstruction of the relict glacial landscape of the Soajo Mountain for the Glacial Maximum Extent (GME) through the following methods: (1) a detailed geomorphological map supported by high-resolution orthophotography, digital elevation models with a spatial resolution of 70 cm, and field surveys; (2) the delineation of the glacial surface, and the calculation of the glacial flowlines

to obtain the numerical model of the ice thickness for the GME; and (3) the estimation of the paleoELA altitudes.

The numerical glacial model of the paleoglacier reconstruction of Soajo as well as the ELA-AABR (Accumulation Area Balance Ratio) values [32] were calculated using the GlaRe (Glacier Reconstruction) and ELA Calculation toolboxes [10,11].

2. Study Area

During the Upper Pleistocene age, all the massifs in the Iberian NW, including Serra del Xistral (1055 m), Faro de Avión (1155 m), Peneda-Gerês (1557 m), Ancares (1967 m), Montes do Cebreiro (1470 m), Courel (1643 m), Manzaneda (1784 m), Teleno (2188 m), and Trevinca (2127 m) (Figure 1a), were dominated by glaciers. These mountains are medium-high reliefs located between 41°30' N and 43°25' N, with relative proximity to the ocean. The northwest Iberian ranges can be divided into two main relief units: the oceanic group, with the lowest mountains located to the west, and the continental group, with the highest ones to the east. However, all these massifs act as a continuous orographic barrier to the westward flow, specifically to the passage of polar fronts.

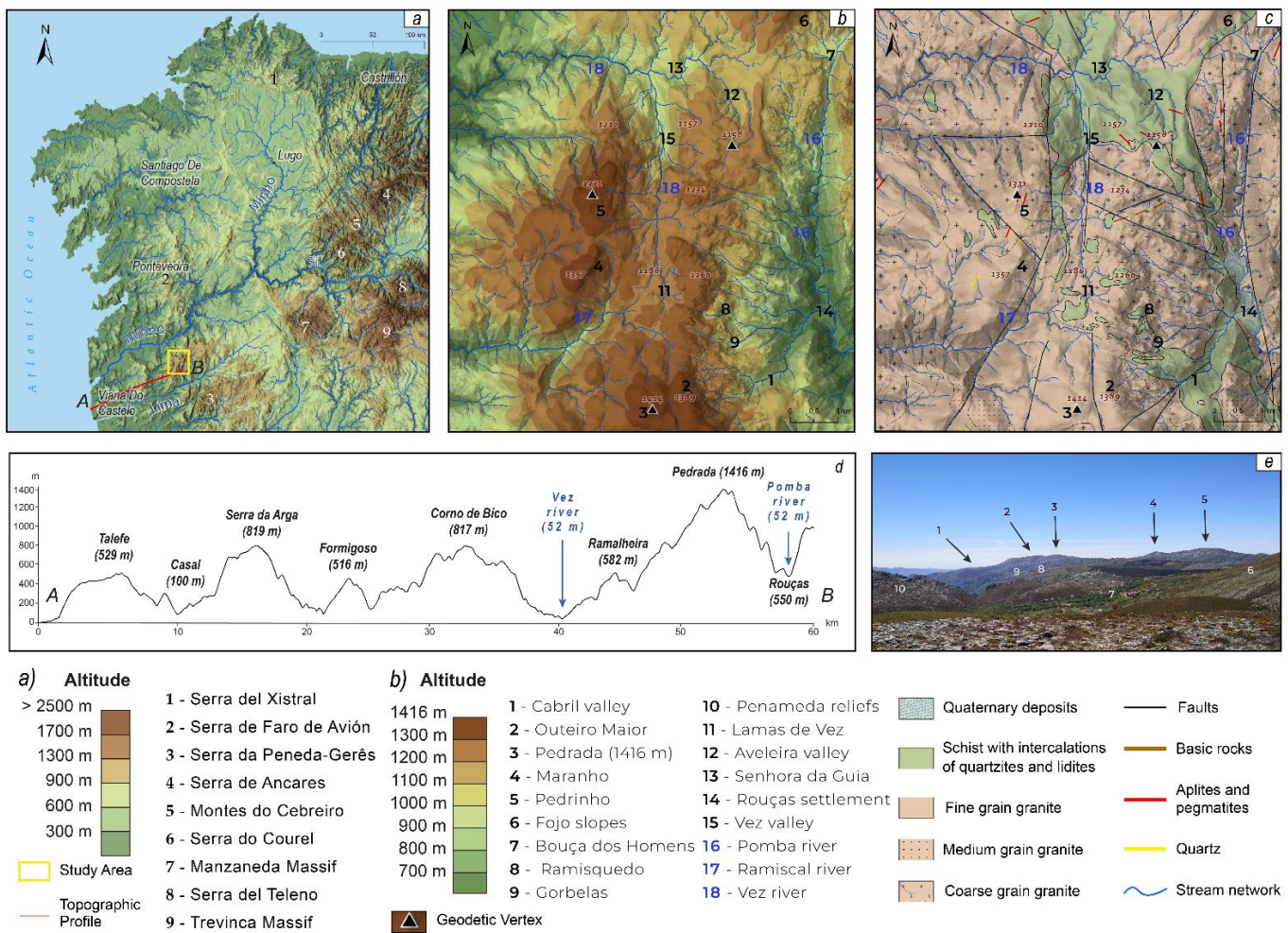


Figure 1. Geomorphological and geological setting of the Serra do Soajo: (a) the mountain massifs of northwest Iberia; (b) cross-section profile (W-E) from the Atlantic Ocean to the Serra do Soajo showing the ascending mountainous relief characteristic of the North of Portugal; (c) hypsometry of the study area; (d) geological map of the study area vectorized from LNEG geological charts 01-B and 01-D; (e) panoramic view of the Serra do Soajo; photo taken from NE, on the geodesic vertex of Fojo at 1289 m (Sources: CIM, 2018; Natural Earth Data, 2022; Diva GIS, 2022; DEM EU Copernicus 25M, 2022; National Laboratory of Energy and Geology (LNEG), 2022).

Serra do Soajo, with its highest peak at 1416 m (Pedrada summit), is located about 50 km from the Atlantic Ocean. It is the closest mountain of significant elevation to the oceanic mountains in the northwest region of Iberia that were affected by glaciers. The neighbouring mountain range of Peneda-Gerês also shares a similar glacial history [33]. In Figure 1b, we can see the mountain staircase that runs from the ocean to the east and ends at the Soajo-Peneda-Gerês massif. This orographic barrier causes the sudden rise and cooling of air masses, which in turn leads to condensation and high levels of total annual precipitation of around 2200 mm [34]. Soajo has a Mediterranean climate characterised by huge contrasted seasons, having seven months (from October until April) with more than 300 mm of precipitation, and the remaining months registering less than 200 mm [34]. The general Mediterranean climate is modified by two aspects: high humidity due to the proximity to the Atlantic, and mountain characteristics, marked by cold and humid weather with high levels of precipitation, negative temperatures during several days (below -5°C), and snowfall periods in the winter. During the summer, the climate is dry, with higher temperature gradients between day and night.

Serra do Soajo, along with its neighbouring massifs of Peneda and Gerês, has a unique impact on the region's climate due to its distinctive relief and varying slope orientations. The orographic barrier created by the relief running from south to north (Figure 1c) results in significant topographic and climatic variations in the area.

The north-facing slopes, which account for 71% of the area, are shaded and therefore have higher humidity levels and less sun exposure. In contrast, the south-facing slopes receive more sun exposure and have lower humidity levels. The west-facing slopes, which make up 16.4% of the area, are highly exposed to Atlantic air masses that rise due to the stairwell topographic profile from west to east. The east-facing slopes, which account for 11% of the area, receive less sunlight and therefore retain snow coverage more easily.

Soajo mountain has a complex shape that roughly resembles a rectangular configuration, measuring 11.26 km in length and 8.12 km in width (Figure 1c). It features an elevation gain of 866 m between the Pedrada summit (1416 m) and the Rouças settlement (550 m). Approximately 18.7% of the massif, or a 140 km² area, has slopes greater than 30°. The mountain can be divided into four main sectors: (1) the three main elevations (Maranho-Pedrinho, Pedrada, and Fonte do Vido); (2) the parallel valleys and slopes to the east; (3) the deep parallel valleys to the west; and (4) the central plateau sector, which is a high depression where the Vez and Ramiscal basins develop. This central plateau sector is then continued northward by the wide valley of the river Vez. The area is characterised by numerous valleys and waterways with a rectilinear configuration, and the drainage network exhibits orthogonal and parallel patterns, indicating the structural conditioning of the relief.

The predominant bedrock in the area is composed of fine- and medium-grained granite with two micas (Figure 1d) and coarse- to medium-grained porphyroid granite, biotitic, and with orbicular facies. Along with granite, the area also contains metamorphic rocks such as schists, hornfels, and metaquartzites, which are mainly oriented NNW-SSE [35]. The relief is strongly influenced by the fracture network, with the primary fracture system in the region exhibiting a perpendicular net of discontinuities with SN-S, NW-SE, W-E, and NNE-SSW orientations, which are mainly related to the old deformation of Hercynian age.

3. Materials and Methods

3.1. Materials

Data from the bibliography, office interpretations, and fieldwork were used to assess the geographic distribution of glacial morphologies in the Serra do Soajo. The field survey, supported by the mobile application Survey123 (<https://survey123.arcgis.com/>, accessed on 15 April 2020), enabled rapid comparisons between office interpretations and field observations, as well as the characterization of glacial landform attributes, such as length, width, and height, as well as the inherent geomorphological processes, coordinates, and photographic records.

The study used LiDAR point cloud data (2.37 pts/m²) collected in 2018 for the Minho Intermunicipal Community (CIM), which permitted the generation of a 70 cm pixel-sized Digital Terrain Model (DTM) and Digital Surface Model (DSM). For the calculation of Digital Elevation Models (DEMs) with LiDAR point clouds (595,118,494 points), 35 laz files were merged into a single LiDAR dataset. To calculate the DTM, we selected those points corresponding to the *Ground* classification code and the *Last* and the *Last of many* as return values. For the DSM calculation, all the classification codes were defined, excluding the *Noise* and the *Reserved* ones. Regarding the return values, all point cloud returns were used. For both DTM and DSM rasters, the *Elevation* attribute was selected. We also used ortho-rectified images acquired in 2004–2006, 2018, and 2021 provided by the Portuguese National Geographic Information System (SNIG, <https://snig.dgterritorio.gov.pt/>, accessed on 25 October 2021), with a spatial resolution between 1 m and 25 cm. Considering the geological context, 01-B and 01-D geological charts (1:50,000) were accessed through the geoportal of the Portuguese National Laboratory of Energy and Geology (LNEG, <https://geoportal.lneg.pt/>, accessed on 18 March 2020).

The glacial mapping for Serra do Soajo followed the geomorphological legend of Lausanne University [36], with an emphasis on the glacial cirques and lateral–frontal moraine ridges that have the greatest significance for paleoglacial reconstructions, as they provide robust data to delineate the former glacial surface [10].

3.2. Paleoglacier Reconstruction

As is typical in paleoglacier reconstructions [10,16], geomorphic evidence such as lateral–frontal moraines and aligned erratic blocks was required to determine the geometry of glaciated areas. The high-precision field and extensive laboratory work led to high-precision hypsometric glacier reconstructions [7].

The altitude values were taken from the high spatial resolution DTM for the significant locations that were identified during the field surveys as erratic blocks and moraine ridges corresponding to the glacier’s maximum ice thickness, i.e., located at higher and further positions of the glaciated area. Paleoglacial ice thickness was calculated using the Glacier Reconstruction (GlaRe) toolkit described in Pellitero et al. [11]. This tool is written in Python 2.7 and is available for ArcGIS versions up to 10.5. GlaRe, among other paleoglacial reconstruction tools such as Volta [37], has the advantage of being able to do strong calculations in GIS environments to accomplish ice thickness estimates. Furthermore, the output is a raster dataset comprising estimates for the ice thickness, which is quite important to calculate the ELA based on the AABR method. The toolbox is a reliable and user-friendly method for ice thickness calculations based on Schilling and Hollin’s [38] equation:

$$h_{i+1} = h_i + \frac{\tau_{av}}{F_i \rho g} \frac{\Delta x}{H_i}$$

“... where h is ice surface elevation, τ_{av} is basal shear stress (in Pa), F is a shape factor, ρ is ice density ($\sim 900 \text{ kg m}^{-3}$), g is the acceleration due to gravity (9.81 ms^{-2}), Δx is step length (in m), H is ice thickness (in m), and i refers to the iteration (step) number.” [11] (p. 2)

According to Patterson [39], this equation considers the perfect plasticity of ice rheology, which means that when ice moves, it responds dynamically to the bedrock as well as its own weight. As stated by the premise of ice rheology, the rate of ice deformation varies with the amount of stress applied to a certain surface [40].

3.3. Equilibrium-Line Altitude (ELA) Calculations

The paleoclimatic significance of the ELA is that it translates the climatic conditions for glaciers to advance or retreat across the glacial stages, oscillating with mass balance [41]. The ELA is the altitudinal line where the net balance ratio is zero [42]. For the ELA calculations, there have been several methods developed over the past century [43–45]. The use of the Maximum Elevation of Lateral Moraines (MELM) and the Accumulation Area

Ratio (AAR) were the two most commonly used approaches for calculating ELA [46–50] until the development of the more current method, the Area/Altitude Balance Ratio (AABR) [51].

In order to achieve the ELA values for the Serra do Soajo, the ELA Calculation Toolbox was used, developed for ArcMap 10.1 software by Pellitero et al. [10] (<https://github.com/cageo/Pellitero-2015>, accessed on 14 April 2022). This toolbox gives the user the option of calculating the ELA according to AABR, Accumulation Area (AA), Accumulation Area Ratio (AAR-Median Altitude), and AAR based on MGE.

In contrast to the AAR method, which uses the total glacial accumulation area and ratio to determine the ELA value, and other methods, such as MELM that considers the lowest glacial deposit, and Toe to Headwall Altitude Ratio (THAR) [52], which relies on the toe and headwall altitudes of the glacier, which can be challenging to define when the glacier is no longer active, the AABR method stands out as a reliable and robust approach for topography-controlled glaciers, considering the paleoglacier hypsometry as an input to calculate the mass balance gradient [52].

The ELA-AABR values can be calculated using the mass glacier balance model generated with the GlaRe toolbox using the following equation:

$$BR = \frac{Z_{ac}A_{ac}}{Z_{ab}A_{ab}}$$

where Z_{ac} is the area-weighted mean altitude of the accumulation area; A_{ac} is the area of accumulation; Z_{ab} represents the area-weighted mean altitude of the ablation area; and A_{ab} is the area of ablation [32].

The ELA-AABR method was applied based on the “representative” Balance Ratio (BRs) values for mid-latitude maritime mountains between 1.7 and 2.0, studied by Rea [51] using the World Glacier Monitoring Service (WGMS).

4. Results

The new geomorphological map is based on 339 field survey points that were used to validate and map glaciogenic landforms along glacial accumulation or ablation areas. By combining field and office work, the researchers identified a range of features, including 3 classic “U”-shaped valleys, 1 icefield, 17 cirque headwalls, nivation nests, polished and striated bedrock, *roche moutonnée*, 122 moraine ridges, and 26 glacial till sites with thicknesses ranging from 0.5 to 4 m. Additionally, 37 locations were identified as dominated by periglacial processes.

These glacial landforms and deposits allowed for the development of the geomorphological map depicted in Figure 2, where it is possible to define three principal sectors: the Lamas de Vez Icefield (LVI), the Vez and Avelira glacial valleys (VAV), and the Eastern Glacial Sector (EGS). Facing west, we have the small glacial valley of Branda da Gémea, which, despite its distance from the main glaciated area, has clear glacial remains. Obviously, the glacial masses had a major effect on the reworking of the landscape, especially in the upper Soajo and eastern valleys and slopes. The glacial conditioning is demonstrated by the abundance of erosional landforms such as small U-shaped valleys, cirques, and polished surfaces, as well as depositional features such as moraines, erratic blocks, and tills.

Globally, the glaciated area is asymmetrical, with coverage extending across the high plateau and a connected tongue in the central area of the mountain. A staircase of multiple coalescent glacial cirques with small tongues can be found to the east, while isolated cirque glaciation can be seen on the west side of the massif. The valleys in Serra do Soajo share similar topographical characteristics. However, this paper focused on four specific valleys—Vez, Cabril, Gorbelas, and Ramisquedo—with lengths ranging from 1.5 to 4 km and a maximum depth of 747 m.

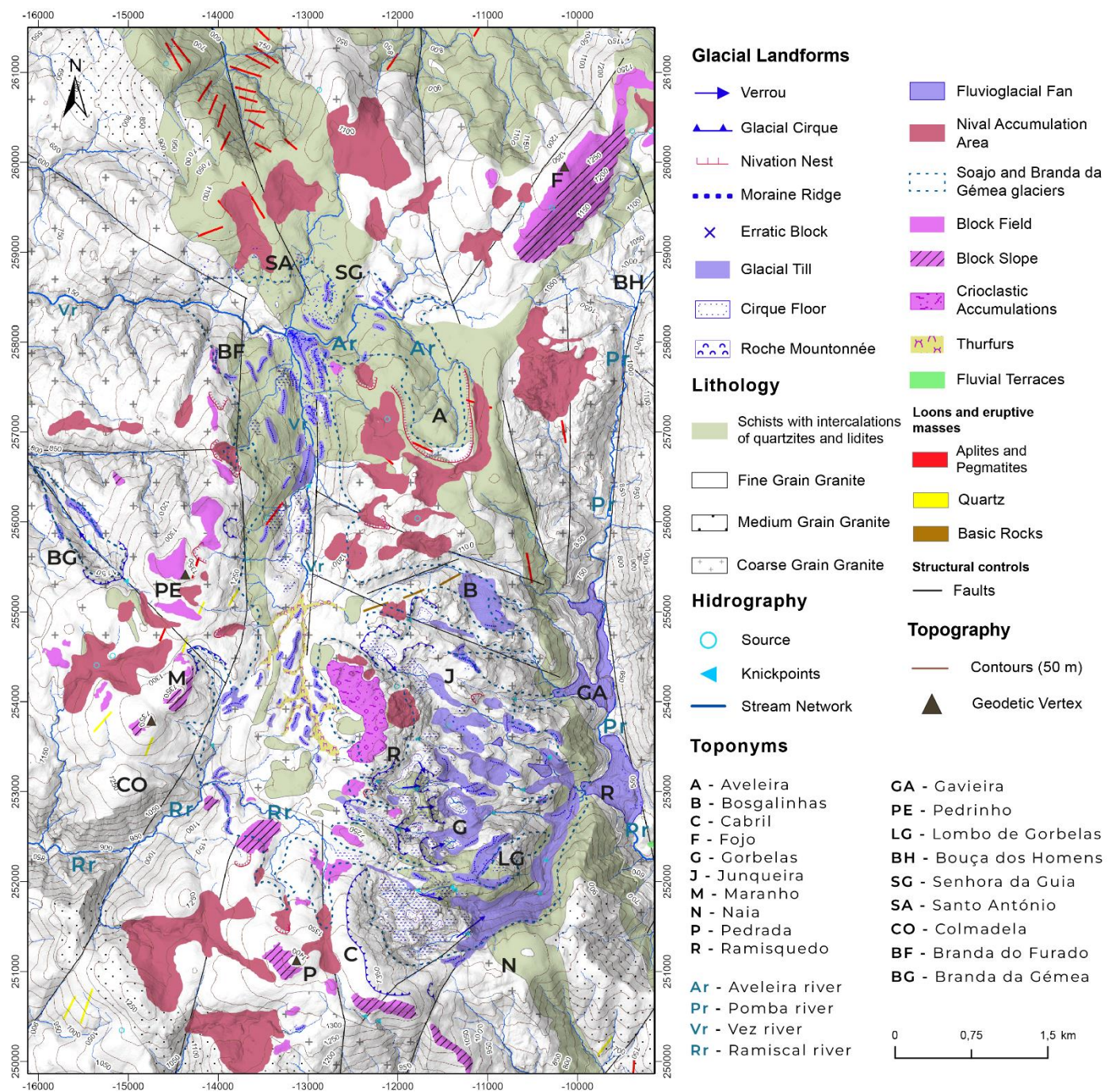


Figure 2. Geomorphological map of Soajo considering the Glacial Maximum Extent (SGME). Some of the main glacial features were already identified in the previous works [19–21,26,29–31] Sources: CIM, 2018; National Laboratory of Energy and Geology (LNEG, 2021).

As a result, there is a noticeable contrast between the glacial and fluvial landscapes in the area. In the Vez Valley, the most significant glacial deposits are located at an altitude of 895 m. In contrast, at Cabril, Gorbelas, and Ramisquedo, the glacial deposits are typically found between 600 m and 650 m of altitude. On the steepest slopes of these valleys, it is common to find dismantled moraines and slope deposits resulting from gravitational processes.

Glacial abrasion effects can be observed in all the aforementioned valleys beginning at an altitude of 1000 m. At these elevations, the exposed bedrock, particularly where granites are dominant, appears to be remarkably smooth and regular, featuring striated

bedrock, and polished rock surfaces and minerals. In contrast, residual granitic reliefs are almost absent.

On the cirque's floors or in the direction of the ice flow are commonly found *roche moutonnée*, striated and polished bedrock, and mineral veins, mostly quartz and feldspar, since granites are the dominant lithology. These landforms related to glacial erosion are frequent at higher altitudes, where the ice promotes higher shear stress. The weathering of the bedrock by cryoclastic and gelifraction processes [53], followed by an intense fracture system with a perpendicular net, created a favourable geological context to exploit all types of weaknesses in the bedrock, leading to a great supply of rocky material to develop well-formed moraine ridges topped by large blocks. It is evident in Figure 2 that ice flow explored the fault network, such as the Vez river tectonic corridor (N-S), as well as the WNE-ESE faults that guided the development of the eastern valleys, facilitating their ice feeding from the central plateau. In the metamorphic basement affected by the ice flow, it is common to observe polished surfaces and clear erratic blocks of huge diameter (approx. 5 m).

The presence of moraines at different altitudes reflects the existence of various tongues besides the GME. The different levels and positions correspond to the retreat of the ice cap, suggesting the occurrence of several phases of (de)glaciation. The largest location of glacial moraines, in Lamas de Vez, vividly displays the radial and dendritic effects of the spatial distribution of glacial mass during the GME. This is due to the connection between the icefield and the neighbouring valleys.

In the Eastern Glacial Cirques sector, the concave granitic shapes between Cabril and Bosgalinhas were covered by ice, with coalescent glacial tongues reaching Rouças and Gavieira. In the northern sector, there is clear connectivity between the Vez and Aveleira glaciers. In most sectors, the moraine ridges are located in the interfluvium, indicating long-lasting glacial accumulation. The identified moraine ridges and erratic boulders are located at varying altitudes, with some at higher positions than others.

Examples of glacial sediments include the sedimentological profiles of Vez lateral moraines, which have deposit thicknesses ranging from 1.8 to 2.1 m and are classified as lodgement and supraglacial melt-out tills at an elevation of 920 m [29]. Another instance is the lateral moraine of Gorbelas/Junqueira at an altitude of 927 m [21,29], which has a thickness of 2.5 m.

On the eastern slopes, fluvio-glacial deposits predominate and are well preserved. Even though Rouças and Gavieira have human settlements, they are primarily made up of enormous granitic stones that are over 8 m in diameter and mixed with sand. While the fluvio-glacial fan at Gavieira (630 m) is confined by the constriction of the Pomba river valley floor, the fan at Rouças (550 m) has a radial shape. These fluvio-glacial landforms are located at the snouts of both locations where intense fluvio-glacial discharges occurred. At the junctions of the tributary valleys of Rouças and Gavieira, small lobes were interpreted as fluvio-glacial masses of weaker glaciations than GME.

The cold and dry climate also left traces related to cryoclastic processes of bedrock weathering, mostly on the western slopes that were exposed to the cold fronts. The mapped periglacial remains were classified as block fields and block slopes. The block field occurs at the peaks or in plain areas, while the block slope occurs where the slope angle is higher, having a greater occurrence at altitudes over 1150 m. The study area is worth mentioning for the relief peaks of the Pedrada, Maranhão, Pedrinho, Fojo, and Outeiro Maior sites. At Pedrada, Maranhão, and Outeiro Maior headwaters could be seen a 2–3 m tall wall with a 5 km of length to trap wolves that could threaten the cattle in the highlands and small shelters for cattle and shepherds, where local communities use the periglacial slabs.

To detail the field data that formed the basis for the calculation of GME and ice thickness, we present detailed observations and data for key sectors.

4.1. Lamas de Vez Icefield

Lamas de Vez's highland area defines a depressed area between 900 and 1200 m of altitude. It is topographically protected by the southern, western, and eastern reliefs, which range between 1416 and 1200 m. The Lamas de Vez highland is a broad and relatively large area (approximately 4 km²). This basin's sheltered location promoted glacial accumulation and led to the formation of an icefield that, at its capacity, nourished the neighbouring valleys in the north, southwest, and east directions.

In this area, there are several remnants of the glacial outflow, including (1) moraine crests formed in the Vez glacial valley at an altitude of 1150 m (Figures 2 and 3a–c); (2) roche moutonnée, striated and polished bedrock (at 1210 m), located between the icefield cells towards the eastern valleys (Figure 2); (3) southwest lateral moraine ridges mostly deposited by the interfluve line in the piedmont of Maranhão (Figure 3a,c,d); and (4) Pedrada piedmont moraine M4 (Figure 3a) towards the Ramiscal valley at an altitude of 1140 m.

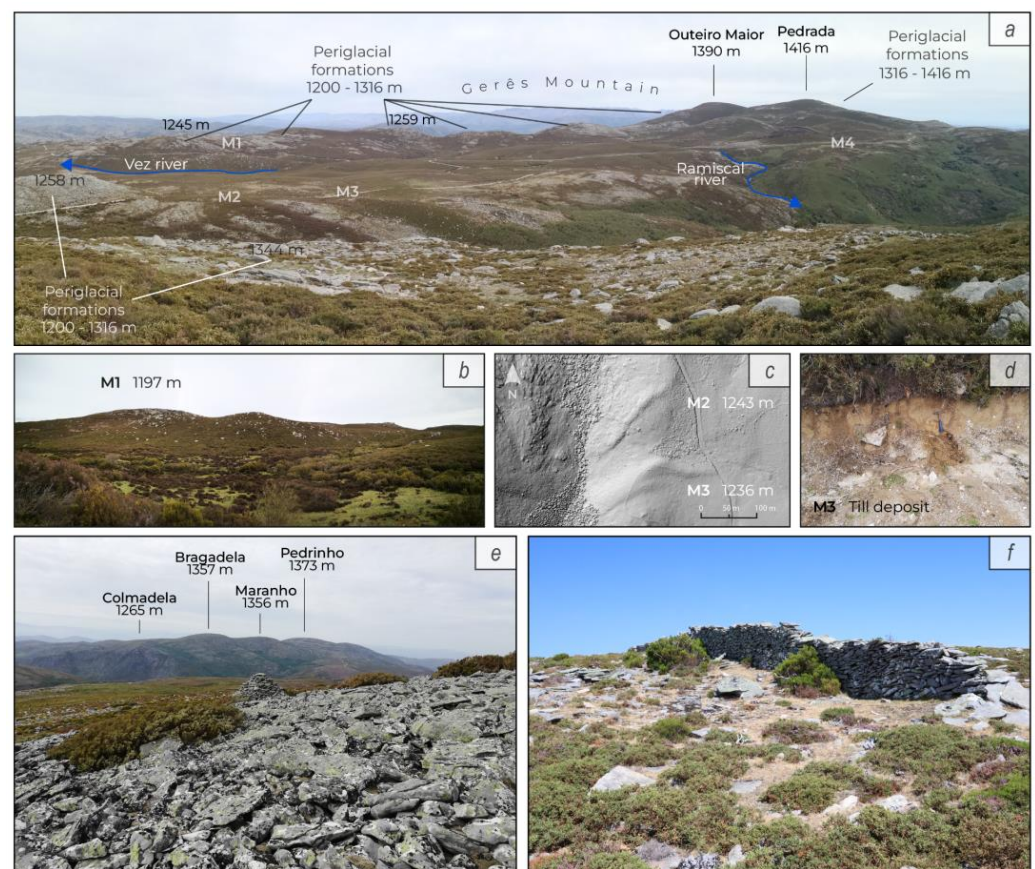


Figure 3. Geomorphological framework of Lamas de Vez sector: (a) global perspective of the icefield plateau, showing several retreat moraine ridges; (b) detailed view of a retreat moraine ridge (M1) and the depression filled with peat bog; (c) detailed view of retreat moraine ridges (M2 and M3) associated with the Ramiscal ice tongue; (d) subglacial till deposit observed on the moraine ridge M2; (e) periglacial blockslope of the northwestern slope of Pedrada; (f) detailed view of a human-made wall with periglacial slabs to catch wolves near the Maranhão peak (local name of Fojo).

Between Maranhão and Pedrada's northern slopes, six parallel moraine ridges were identified. The three lateral moraines near Maranhão registered altitudes between 1240 m and 1230 m (Figure 3d). The others, located at the Pedrada piedmont, range between 1177 m and 1115 m (Figure 3e).

At an altitude of 1200 m, the highland of Lamas de Vez is characterised by its wide-open, depressed morphology and spans almost 4 km². This location is the primary topographical factor for snow and ice accumulation in the area, having previously acted as a flat

surface that led to the formation of an icefield. Today, Lamas de Vez is the head catchment for the Ramiscal and Vez rivers.

4.2. Glacial Valleys of Vez and Aveleira

Lithologically, these two valleys are similar. Both registers have patches of metamorphic basement appearing between granitic bedrock. Here, the valley glaciers were easily explored for structural pattern and weaknesses, with the current profile of both defined as “U”-shaped valleys (Figure 4a,b). The observation of the highest right-sided erratic block of Vez Valley was extremely clear, located at 1069 m of altitude (Figure 4a,d). Boulderated moraine ridges were discovered at 1000 m altitude in Senhora da Guia and Aveleira valleys, where it is common to find granitic erratic blocks having dimensions >10 m in diameter, deposited between 1025 and 976 m of altitude, distributed along the slopes (Figure 4a,f).

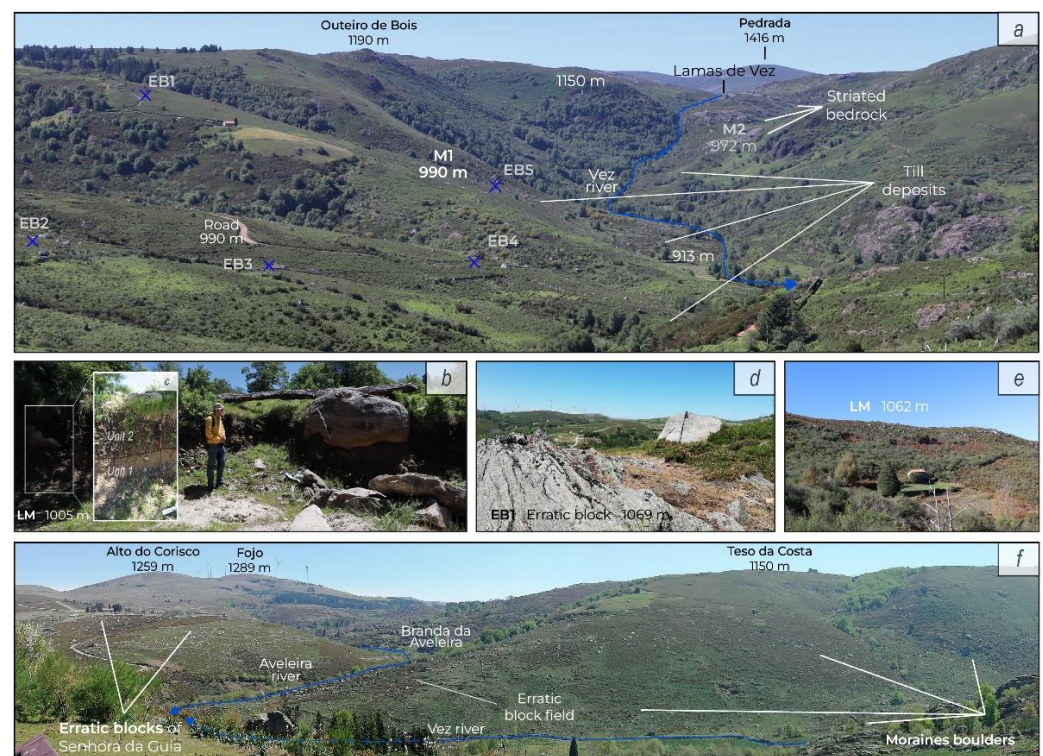


Figure 4. Geomorphological framework of Vez and Aveleira glacial valleys and marginal glaciated areas of Santo António and Senhora da Guia: (a) “U” shaped Vez valley and the distribution of moraine ridges located in Vez and Aveleira valleys and Senhora da Guia; (b) lateral moraine (LM) in Aveleira valley; (c) glacial diamicton showing Unit 1: slope deposits, and Unit 2: clayey-coarse grained till with erratic metric block; (d) granitic erratic block (EB1) deposited over schist outcrop in Vez Valley; (e) lateral moraine (LM) in Branda do Furado; (f) panoramic view of moraines boulders at the marginal sector of Vez glacial valley and erratic block field at the confluence area between the Vez and Aveleira rivers.

4.3. Eastern Glacial Sector (EGS)

The EGS area is characterised by a significant glacial sub-excavation surface, which is directly related to the bedrock’s structural conditions dominated by perpendicular fracture systems in different directions (S-N, W-E, SE-NW). The glacial erosion process contributed to weakening of the granitic bedrock, resulting in concave physiognomies in classic armchair-like shapes in the form of cirque glaciers [40] (Figure 5a). These glacial cirques, situated between 1300 m and 1000 m of altitude, exhibit a staircase topographic profile of the eastern valleys, where the apex of one cirque forms the lip of its consecutive (Figure 5a). The intense erosional processes resulted in abundant rocky material, forming most of the moraine ridges identified in the eastern sector.

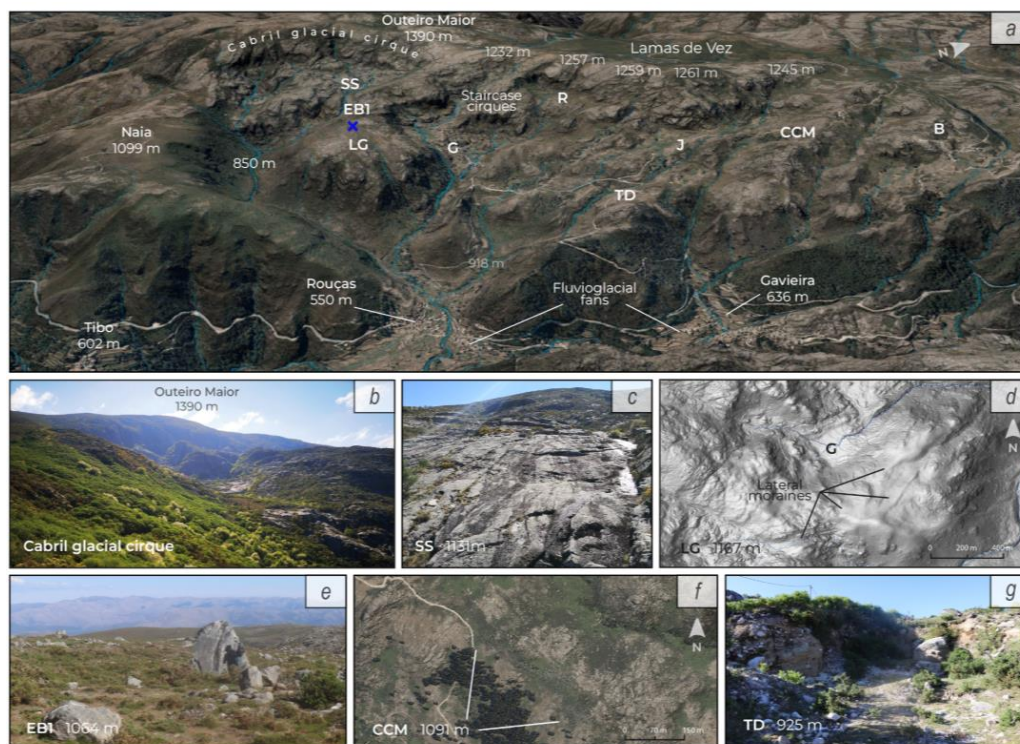


Figure 5. Glacial geomorphology of the Eastern Glacial Sector of the Serra do Soajo: (a) geomorphological perspective of the glacial cirques, valleys, and deposits at Lombo de Gorbelas (LG), Gorbelas (G), Ramisquedo (R), Junqueira (J), and Bosgalinhas (B), and fluvioglacial deposits at Rouças, Gavieira settlements (orthorectified imagery from SNIG and LiDAR DSM); (b) Cabril glacial cirque with wide amphitheatre; (c) striated and polished surface (SS) in Cabril glacial cirque; (d) hillshade representing lateral moraines deposited at Lombo de Gorbelas (LG); (e) erratic block (EB1) deposited at LG; (f) Casa do Cavalo moraine (CCM) deposited by the interfluve line at Junqueira settlement; (g) till deposit (TD) exposure near Junqueira settlement.

The outlet of the Cabril glacial cirque at 1100 m of altitude (Figure 5a,b), Lombo de Gorbelas (Figure 5d), and Ramisquedo slopes between 1074 and 1021 m of altitude (Figure 5a,c) feature boulder lateral moraine ridges. The most prominent moraine is situated at Casa do Cavalo, measuring 322 m in length and deposited at an altitude of 1090 m (Figure 5a,f).

At the EGS, the distribution of depositional glacial landforms starts between 1100 m and 1000 m of altitude, right after the glacial accumulation areas. The Cabril valley, one of the greatest glacial valleys of Serra do Soajo, has fewer deposits that can help us understand how intense the fluvioglacial discharge was. At the EGS, the moraine ridges are specially deposited by the interfluve lines of different valleys, which is strong evidence for the glacial coalescence of ice tongues. Here, there is a strong contrast with the marginal sections of Santo António and Senhora da Guia in terms of glacial deposits preservation. Morphologically, the glacial deposits found in the EGS are also composed of boulders of great dimensions (mostly granite), and it is possible to identify classic examples of till exposures.

4.4. Branda da Gémea Glacier

Located on the outskirts of the SGME, Branda da Gémea glacial valley, nicknamed Corga dos Cortelhos (Figure 6a) by Coudé-Gausson et al. [20], presents unique topographic and structural conditions. At 1300 m, the cirque's head collides with the base of the Pedrinho peak. The presence of faults with a SE-NW orientation dominates the valley's orientation. The slope's position on the left side facing NE and the right-side facing NW makes them shady slopes. During the Pleistocene glaciations, these variables enabled the

formation of a glacial tongue in the Branda da Gémea valley (Figure 6b). The ice mass in Branda da Gémea could deposit material to form well-defined lateral moraine ridges (Figure 6a,c) with a length of about 450 m deposited between 1105 m and 950 m of altitude.

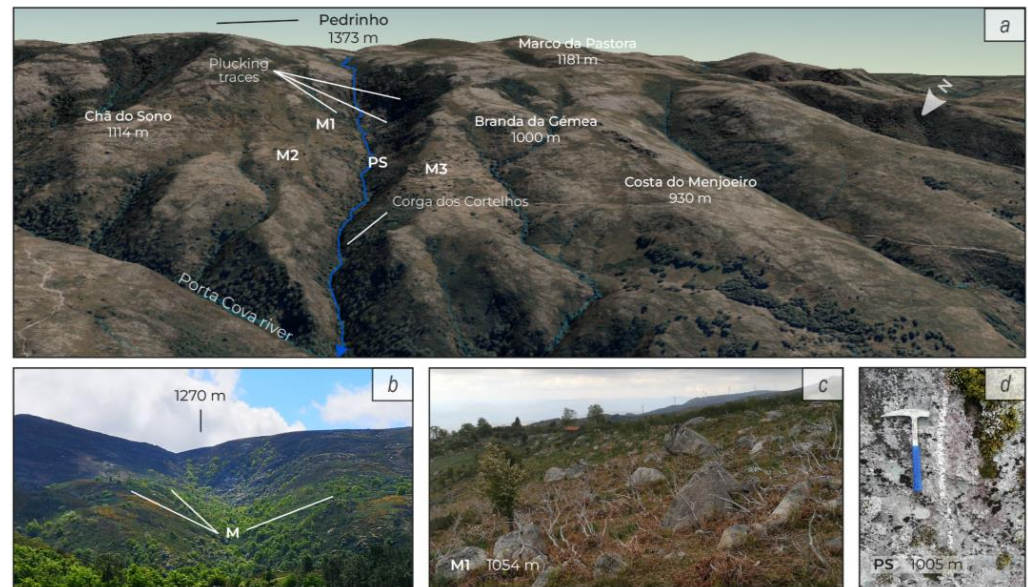


Figure 6. Glacial geomorphology of Branda da Gémea valley: (a) three-dimensional panoramic view of Branda da Gémea and neighbouring valleys (orthorectified imagery from SNIG and LiDAR DSM); (b) Branda da Gémea glacial valley, cirque, and lateral moraines (M); (c) dismantled lateral boulder moraine (M1) with lack of glacial diamicton by the right slope of the valley (M1); (d) polished granitic surface (PS) at Branda da Gémea.

4.5. Glacier Surface Reconstruction

Glacial Maximum Extent and Ice Thickness

Globally, the reconstructed model of the Soajo Maximum Glacial Extent (SGME) revealed a radial distribution of the glaciated area and an isolated tongue on the west, developed along the Branda das Gémea valley (Figure 7). The recreated paleoglacier surface covers c.a. 16 km² and depicts how the glacial flow would have been across the valleys throughout the GME (Figure 7).

The Lamas de Vez icefield was the main feeder for the propagation of the glacial tongue along the Vez valley towards the north. Moraines and erratic blocks belonging to the Aveleira valley's glacial tongue justify the coalescence of glacial tongues that occurred in this frontal sector. In the SW sector of the icefield, the Ramiscal valley also benefited from the glacial outflow. The lateral moraine found between Maranhão and Pedrada (Figure 3a,c) supports this interpretation. In the Branda da Gémea glacial valley, despite the disassembled appearance of moraine crests, these are interpreted by the longitudinal alignment of erratic megablocks and the absence of glacial diamicton.

The model most likely replicates the ice thicknesses in the accumulation zones (Lamas de Vez icefield, glacial cirques headwalls of Branda da Gémea, and eastern glacial sectors) and the ablation zones (Santo António, SW of Ramiscal drainage, Rouças). The icefield of Lamas de Vez had ca. 3.30 km² of area, representing 20% of the total glaciated area, with a volume of 214.4 hm³ and a maximum ice thickness of 127 m (Table 1).

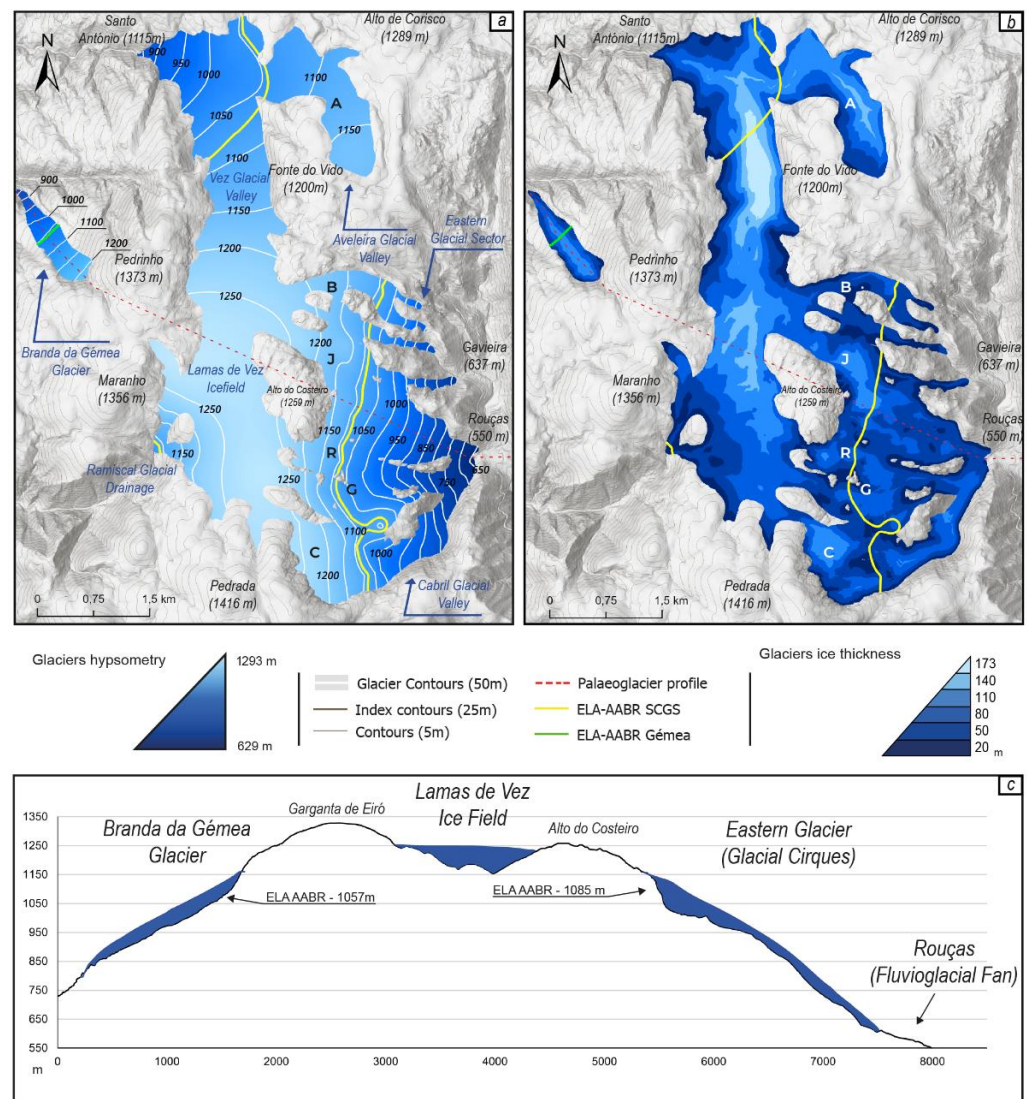


Figure 7. Soajo Glacial Maximum Extent reconstruction: (a) hypsometry of the glaciated areas (C—Cabril; G—Gorbelas; R—Ramisquedo; J—Junqueira; B—Bosgalinhas; A—Aveleira); (b) ice thickness surface of the glaciated areas; (c) topographic profile (approx. ENW-ESE) with the respective ice thickness (Source: CIM, 2018; ELA Calculation Toolbox, 2015; GlaRe Toolbox, 2016).

Table 1. Spatial measures for each one of the glacerized sectors in Serra do Soajo for Glacial Maximum Extent (GME).

	LVez If	VeZR v	Avel v	SW Ram S	Cab v	EGS	Total	BGem v
Glaciated area (km ²)	3.305	3.968	1.55	0.714	1.859	5.1	16.496	0.419
Glaciated area (%)	20	24	9.4	4.3	11.3	31	100	100
Max. ice thickness	ca. 127	173	118	66	106	107	-	110
Ice volume (hm ³)	214.4	269.2	115.8	14.6	79.0	188	881.2	24.3
Ice volume (%)	23.7	29.7	12.8	1.6	8.7	20.8	100	100
Length (km)	2.86	2.92	2.98	0.7	3.3	2.99	-	1.92
Max. altitude (m.s.l.)	1250	1247	1157	1274	1256	1210	-	1217
Min. altitude (m.s.l.)	1150	830	1033	1060	737	649	-	796

LVez If—Lamas de Vez Icefield, VeZR—Vez river valley, Avel v—Aveleira valley, SW R S—SW Ramiscal sector, Cab v—Cabril valley, EGS—Eastern glacial sector, BG v—Branda da Gémea valley.

Due to the icefield supply, the Vez glacier receives and accumulates a significant volume of ice, which leads to an accumulation of ca. 269 hm³. The Aveleira Valley headwaters are at 1169 m in altitude and are oriented to the north and later to the west (Figure 7). The glaciated area of the nivation nest and valley glaciers that developed here is 1.55 km², accounting for 9.4% of the overall area. The greatest thickness, according to the computed model, is 118 m. The volume in this section is 115 hm³ (Table 1).

The glaciers in the SW sector of Lamas de Vez attained maximum thicknesses of 66 m, 700 m in length, and 15 hm³ in volume, accounting for approximately 2% of the total ice volume measured in the studied area (Table 1).

The iterated glacial model of the EGS had an area of 5 km². They developed well until they approached the snouts (Gavieira and Rouças), with ice thickness varying between 107 and 18 m from the higher to the lower altitudes of the valleys. The distribution of moraines and erratic blocks showed a dendritic behaviour between the former glaciers during the GME, particularly between 1150 m and 750 m. The ice tongues were not thicker than 107 m. They covered 5.1 km² and accounted for 31% of the entire glaciated surface. The volume was estimated to be around 188 hm³. The glaciers that evolved in these valleys were around 3 km long (Table 1).

The Cabril valley ice tongue stands out among the eastern glaciers for its size, with an area of 1.9 km², constituting 11.3% of the overall area of the SGME. It has a calculated volume of ca. 79 hm³ and a maximum thickness of 106 m, reaching a length of ca. 3.3 km (Figure 7b). Branda da Gémea glacier was calculated separately from SGME. The glacial model appropriately corresponds to the previously observed and discussed moraine ridges. According to the calculated surface (Figure 7a), the Vale da Branda da Gémea glacier reached around 2 km in length and 0.41 km² in area. In volumetric terms, the glacier attained a maximum thickness of 110 m, and the glacial basin held approximately 24 hm³ of ice.

Lamas de Vez icefield and Vez glacier revealed similar area percentages (20–24%) and registered the greatest volume percentages (29.7–23.7%). These values help to understand how glacial accumulation dynamics were active and intense, firstly due to the orographic barrier between Maranhão-Pedrinho-Alto da Preguiça (S-N), and secondly because of the icefield glacial outflow.

The Aveleira glacier has the same behaviour in area and ice thickness as the Vez glacier proportion, but with lower values. The SW Ramiscal, Cabril Valley, and Eastern glacial sectors show that glacial tongues had greater glaciated areas than ice thickness percentages (lower than 5% on both metrics). The Eastern Glacial Sector reveals the biggest glaciated area, with more than 30% of the total glacial surface in Serra do Soajo, but it is 8.9% thinner than the Vez glacial tongue.

The radial effect on glacier distribution during the SGME shows that the passage of polar fronts, from west to east, promotes ice accumulation more easily on the east-oriented slopes. The same effect of the polar front passage was also noted by Vieira [14] in the Serra da Estrela paleoglacier. The orographic precipitation and topographic features allowed the eastern slopes to promote the development of important glacial masses.

4.6. ELA-AABR Result

For the ELA paleoglacial reconstruction (Figure 7 and Table 2), the Branda da Gémea glacier was calculated separately because it is a simple glacial valley with independent glacial dynamics from the Lamas de Vez icefield. For the valleys connected by glacial drainage from the icefield, the ELA calculations were performed jointly across the entire paleoglacier surface. The ELA-AABR values worked very well (Table 2) with the lateral moraine ridges associated with the GME in Lombo de Gorbelas with altitudes between 1100 m and 964 m and with the Casa do Cavalo lateral moraine located at 1074 m of altitude, which represent the most prominent moraine ridges in the eastern glacial sector. The northern deposition marginal sector of Santo António and Senhora da Guia also revealed a good relationship between the height of the identified glaciogenic features and

the ELA-AABR calculations. Additionally, the values calculated for the northwest valley of Branda da Gémea (1217 m) registered a significant relationship with the moraine ridges located on both valley sides between 1066 m and 958 m.

Table 2. ELA balance ratio for AABR methods for the Soajo Glacier Maximum Extent (SGME) and for the Glacial Valley of Branda da Gémea.

SGME			Branda da Gémea Valley Glacier		
BR	Method	ELA (m)	BR	Method	ELA (m)
1.7	AABR	1100.5	1.7	AABR	1057.5
1.8	AABR	1085.5	1.8	AABR	1057.5
1.9	AABR	1085.5	1.9	AABR	1057.5
2.0	AABR	1085.5	2.0	AABR	1057.5

5. Discussion

The findings of this study highlight two important aspects of the glaciation of Soajo: the distinct shape of the glaciated area within three sectors, and the flow of the glacier from the centre outwards. The reconstruction of the ice-covered area indicates that there were multiple connected glacial basins during the GME, and the glaciated plateau of Lamas do Vez served as the ice source for the surrounding valleys, except for the isolated valley of Branda da Gémea in the west. As a result, the ice cover spread radially, exploiting lithological weaknesses and fractures in the rock. The topographic features of deeply embedded valleys and lowered pathways also facilitated the glacier's flow.

Coudé-Gausson et al. [20] and Pereira and Pereira [26] had already delimited the glaciated area, but the glacial landforms and deposits that supported their map were quite limited. Our systematic fieldwork and the LiDAR data interpretation showed that there are more geomorphological elements to support the definition of the ice-covered surface, the definition of the maximum extent of the ice, and the calculus of the ice thickness.

Several factors contributed to the presence of glaciers in Serra do Soajo, including (1) the N-S orientation of the granite relief that dominates the study area, and its lithological influence on the paleotopographic conditions for the development of ice accumulation surfaces, as well as the dense fractures network that was exploited by the ice erosion and flow [19]; (2) the proximity to the Atlantic Ocean and the climatic influence from the passage of the wet polar fronts combined with the occurrence of an abrupt orographic lift, responsible for abundant rainfall on the mountains windward side and significant snowfall on the mountain highlands, where cold conditions were severe during the winter [2]; and (3) the valley sheltering glacial masses from insolation when orientated from north to east. The same effect was observed by Daveau and Devy-Vareta [54] in Serra da Cabreira, and Santos-González et al. [7] confirmed that in the Iberian northwest, the topographic features are responsible for the development of microclimates at high elevations [8,55].

These factors explain not only the variations between non-glacial slopes oriented W-S (with the exception of SW Ramiscal) and glaciated slopes oriented N-NE-E, but also the abundant accumulation of ice in highlands over 1000 m of altitude.

In the northwest of the Iberian Peninsula, there are several massifs comparable to Soajo in terms of glaciated surface area, number and extent of glacial tongues, and glacial dominance over N- and E-oriented slopes. Comparatively, Serra do Soajo (1416 m—Pedrada summit) had approximately 16 km² of glaciated area, 6 glaciers, and 5.78 km of maximum glacier length. Serra do Courel (1641 m—Formigueiros peak) has a glaciated area of 19.2 km² and 9 glaciers, the longest glacier being 4.8 km [55]; and Serra Faro de Avión (1151 m—Avión peak) has 19.6 km² of glaciated area and 2 glaciers, the longest glacial tongue being 3.4 km [56]. Despite the varying elevations of these three glaciated regions, the former glaciers developed quite well on the north- and east-facing slopes.

Regarding the ice thickness in glaciated areas, the Lamas de Vez Icefield reached 127 m, while the Vez glacial valley reached 173 m. At Serra do Courel, the Seara icefield had a thickness of 130 m, whereas the Ferreirós and Folgoso glaciers had a maximum thickness of

65 m [55]. Valcarcel and Pérez-Alberti [56] and Schmidt-Thomé [57] noted the presence of an icefield and two minor glaciers that drained through the valleys of Cabana and Outeiro in Serra Faro de Avión, but there are no precise data on the ice thickness.

Comparatively, the paleoglaciated regions of Soajo, Faro de Avion, and Courel had nearly identical dimensions and glacier thicknesses, but each developed its own distinctive glacial morphology. This led us to the conclusion that the climatic conditions were very similar, but the relief arrangement provided intriguing features for ice accumulation and erosion, while snowfall intensity was similar.

5.1. NW Portuguese and NW-N Iberia ELA's

Regarding the ELA's variation values in northwest Iberia and for comparative purposes, the values calculated through the AABR and THAR were considered, as they are the most compatible methods. Furthermore, the studies refer to the local Last Glacial Maximum (ILGM), except in the case of Soajo, where the ELA's were calculated for the GME.

Considering the data in Figure 8, the ELA values in the Iberian northwest increase from W-E and from N-S, revealing the exposed nature of the northwest Iberian coastal massifs and the influence of cold maritime conditions. Starting from west to east, the Cantabrian Mountains have a maximum ELA of 1883 m; Serras de Teleno, La Cabrera, and Trevinca have similar ELA between 1830 m and 1833 m of altitude. Serra do Courel and Cebreiro-Oribio Mountains have 1320 m and 1255 m of altitude, respectively, with a difference of 65 m between them.

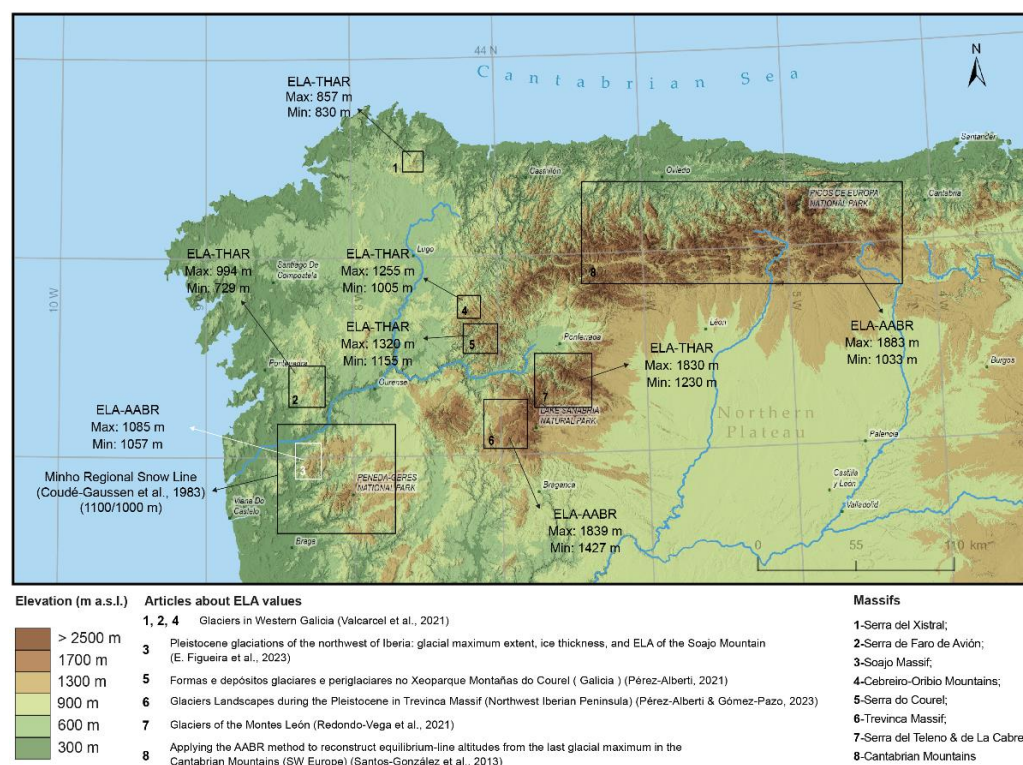


Figure 8. Comparison of the ELA values obtained in this study and in other research works for northwestern Iberia (Sources: SRTM 90 m, 2022; Natural Earth Data, 2022) [7,17,20–22,29,56].

Concerning the maximum values (Figure 8), the western massifs of northwest Iberia have the lowest ELA values, starting with Serra del Xistral (857 m), then Serra de Faro de Avión (994 m), and then Serra do Soajo (1085 m).

Comparing the results of this study with those of Cantabrian Mountains, which have an altitude of 2411 m [7], the distribution of the ELA drops in altitude analogously from the internal areas towards the ocean.

In Serra do Soajo, ELA altitude values range between 1057 m and 1087 m, and this variation between mountain sides can be explained by the inner and less-exposed position of Soajo than Branda da Gémea to humid westerly or northerly winds such as the Cantabrian Mountains ELA variation [7].

The spatial comparison of ELA values between these locations is defined not only by the climate conditions during the Upper Pleistocene cold periods but also the microclimates created by the relief arrangement [12,58–60]. The asymmetrical distribution was once described by Coudé-Gausson [19] in a PaleoELA map, reflecting the contours of ELA in the Iberian Peninsula during the LGM.

5.2. Limitations and Further Challenges

Our research findings highlight the need for additional studies in order to have a more reliable paleoglacial reconstruction of the Soajo Mountain, improving our understanding of the glaciation's processes, depositional landforms, stages, extent, and chronology.

The major limitation of the present reconstruction is the lack of dating to establish a chronology of the glaciation, since it only considered the ice cover extent for the GME, to which no date can be given. However, the staggered positioning of glacial landforms and deposits in altitude and along the valley floors indicates the occurrence, at least, of three distinct phases of ice cover retreat.

The presence of distinct lateral moraine ridges and aligned-erratic blocks in the area is indicative of recent glacial/deglaciation stages. Although erratic blocks in the Senhora da Guia (1000 m a.s.l.) and Vez-Aveleira valleys (900 m a.s.l.) sites were recently dated by the ^{10}Be cosmogenic nuclide method [61], yielding, respectively, 22.9 ka and 16.3 ka, pointing to the Last Glacial Maximum (LGM) and Younger Dryas, there are no dating records for many significant places. The recent dates for Serra do Soajo, when compared with the neighbouring massifs of Trevinca and Manzaneda (Figure 8), where Pérez-Alberti and Gómez-Pazo [17] defined four glacial phases based on the available chronology data [13,53,62–65], seem to match the second, between 22 ka to 19 ka, and third categories (16 ± 7 ka), lacking the first (44 to 27 ka) that is supposed to be the GME, and the most recent (16 to 11 ka).

Even with the mentioned limitations, it is noted that the first detailed geomorphological map of the area is presented, an element that will support the definition of the sampling sites for dating in order to perform a chronologically accurate paleoglacial reconstruction. Because of the scientific potential implied in this area, future research should concentrate on the use of absolute and relative dating techniques to establish the chronology of the LGM and all subsequent deglaciation episodes.

Further studies should be developed to understand the paraglacial landscape reaction [66–68], since the location of the glacial landforms and deposits suggests that the Serra do Soajo glaciers melted permanently due to climatic oscillations. As the ice retreated, fluvio-glacial processes ensued, leading to the creation of proglacial environments such as peat bogs at Lamas de Vez, colluviums in the Vez and Cabril valleys, and the fluvio-glacial fans at the EGS that could be promoted by a local Foëhn effect [69]. These non-glacial landforms indicate the transition from the cold-dry/humid climates of the Upper Pleistocene to the warm-dry/humid climates of the Holocene [70].

The majority of the mountain's glacier key locations is readily accessible, however, some valley sections can be difficult to obtain because of the dense vegetation there. The presence of glacial diamictons also contributes to the dense land cover, making it difficult to confirm deposits in some valleys such as Branda da Gémea, Vez, Aveleira, Cabril, and Gorbelas/Ramisquedo valleys. Other structures, such as the erratic block field at the Vez-Aveleira glacial confluence and the left lateral moraine ridge of the Ramiscal valley, still need to be confirmed.

The presence of glacial till at the Bouça dos Homens depression (1053 m) in the west (Figure 2) indicates glacial activity that must be investigated, and the hypothesis of an

ice connection between this area and the Aveleira glacier via the Fonte do Vido passage (1200 m) is another hypothesis to test.

There are distinctive till exposures, fluvio-glacial fans and lobes, gravity landforms, and colluviums in the glacial deposits of the Serra do Soajo. Assuming the current understanding of till deposits provided by Santos et al. [28], future sedimentological investigations will contribute to a comprehensive understanding of the character of glacial deposition and confirm whether or not the deposit has been reworked by external processes. With adequate date records, it may be possible to distinguish their spatiotemporal sequence and characterise deglaciation phases up until their final retreat.

6. Conclusions

The study of paleoglaciers in Serra do Soajo is not new; however, the scarcity of high-resolution DEMs and the lack of detailed surveys has slowed the geomorphological knowledge of the area. This study provides a new detailed geomorphological analysis of the glaciated area and a paleoglacial reconstruction.

Despite the low-lying altitude of the Soajo mountain, it reveals an important geodiversity of glaciogenic landforms. The glacial dynamics of these ancient glaciers were highly sensitive to climate change due to their low altitude. It is essential to comprehend that the mountain glaciers of the Serra do Soajo attained an unusual size despite their low altitude, and they would have easily retreated with small climatic fluctuations.

According to the numerical glacial models of both the Soajo and Branda da Gémea paleoglaciers, the calculated values define the former paleoglaciers' ice thickness and volume for the GME in Serra do Soajo, which had radial and dendritic glacial flow.

The Soajo paleoglacier reached a maximum thickness of 173 m, while Branda da Gémea reached a maximum thickness of 110 m based on GME ice thickness outputs. The calculated volumes of the paleoglaciers Soajo and Branda da Gémea are 881.2 hm³ and 24.3 hm³, respectively. The calculated ELA values correspond well with the lateral moraine ridges, and the ELA altitudes for the Soajo paleoglacier and Branda da Gémea are 1085 m and 1057 m, respectively. These former ELAs intersect the GME-related lateral moraines deposited in glaciated valleys, thereby separating glacial accumulation and ablation zones with relative ease.

During fieldwork, it emerged that anthropic pressure is a persistent and widespread threat to the preservation of glacial landforms and deposits, particularly in locations such as Branda de Santo António, Senhora da Guia, Branda da Aveleira, and Ramisquedo. Due to their scientific significance for geo-patrimonial recognition and classification, as well as for educational and cultural objectives, many of the locations mentioned in this study require geoconservation measures.

Supplementary Materials: The following links are an open-source way to obtain the toolboxes used in this study, as well documentation and videos related to both of them. Link (1): GlaRe toolbox (<https://www.abdn.ac.uk/geosciences/departments/geography-environment/outcomes-442.php>, accessed on 1 May 2021, GlaRe toolbox tutorial (<https://www.youtube.com/watch?v=TOtNesIbm1M>, accessed on 4 May 2021). Link (2): ELA calculation toolbox (<https://github.com/cageo/Pellitero-2015>, accessed on 10 December 2020), ELA calculation toolbox tutorial (<https://www.youtube.com/watch?v=mxNG35SjDtg>, accessed on 13 December 2020).

Author Contributions: Conceptualization, A.G. and E.F.; methodology, E.F. and A.P.-A.; software, E.F.; validation, E.F., A.G. and A.P.-A.; formal analysis, E.F., A.G. and A.P.-A.; investigation, E.F., A.G. and A.P.-A.; resources, E.F., A.G. and A.P.-A.; data curation, E.F. and A.G.; writing—original draft preparation, E.F. and A.G.; writing—review and editing, E.F., A.G. and A.P.-A.; visualisation, E.F., A.G. and A.P.-A.; funding acquisition, A.G. All authors have read and agreed to the published version of the manuscript.

Funding: Alberto Gomes received support from the Centre of Studies in Geography and Spatial Planning (CEGOT) (Grant 2016/19020-0), funded by national funds through the Foundation for Science and Technology (FCT) under the reference UIDB/04084/2020.

Data Availability Statement: The data presented in this study are available upon request from the authors. The data are not publicly available due to size and institutional restrictions.

Acknowledgments: We would like to thank Ramón Pellitero for his assistance during the GlaRe toolbox implementation phases as well as the assistance provided when computing the Equilibrium Line Altitude (ELA).

Conflicts of Interest: The authors declare no conflict of interest.

References

1. Woodward, J.; Hamlin, R.; Macklin, M.; Hughes, P.; Lewin, J. Glacial activity and catchment dynamics in northwest Greece: Long-term river behaviour and the slackwater sediment record for the last glacial to interglacial transition. *Geomorphology* **2008**, *101*, 44–67. [[CrossRef](#)]
2. Owen, L.A.; Thackray, G.; Anderson, R.S.; Briner, J.; Kaufman, D.; Roe, G.; Pfeffer, W.; Yi, C. Integrated research on mountain glaciers: Current status, priorities and future prospects. *Geomorphology* **2009**, *103*, 158–171. [[CrossRef](#)]
3. Palma, P.; Oliva, M.; García-Hernández, C.; Ortiz, A.G.; Ruiz-Fernández, J.; Salvador-Franch, F.; Catarineu, M. Spatial characterization of glacial and periglacial landforms in the highlands of Sierra Nevada (Spain). *Sci. Total Environ.* **2017**, *584–585*, 1256–1267. [[CrossRef](#)] [[PubMed](#)]
4. Pearce, D.M.; Ely, J.; Barr, I.; Boston, C.M. Section 3.4.9: Glacier Reconstruction. In *Geomorphological Techniques*, Online ed.; British Society for Geomorphology: London, UK, 2017; Volume 9.
5. Vieira, G.; Palacios, D.; Andrés, N.; Mora, C.; Selem, L.V.; Woronko, B.; Soncco, C.; Úbeda, J.; Goyanes, G. Penultimate Glacial Cycle glacier extent in the Iberian Peninsula: New evidence from the Serra da Estrela (Central System, Portugal). *Geomorphology* **2021**, *388*, 107781. [[CrossRef](#)]
6. Pellitero, R.; Fernández-Fernández, J.M.; Campos, N.; Serrano, E.; Pisabarro, A. Late Pleistocene climate of the northern Iberian Peninsula: New insights from palaeoglaciologists at Fuentes Carrionas (Cantabrian Mountains). *J. Quat. Sci.* **2019**, *34*, 342–354. [[CrossRef](#)]
7. Santos-González, J.; Redondo-Vega, J.M.; González-Gutiérrez, R.B.; Gómez-Villar, A. Applying the AABR method to reconstruct equilibrium-line altitudes from the last glacial maximum in the Cantabrian Mountains (SW Europe). *Palaeogeogr. Palaeoclim. Palaeoecol.* **2013**, *387*, 185–199. [[CrossRef](#)]
8. Oliva, M.; Palacios, D.; Fernández-Fernández, J.; Rodríguez-Rodríguez, L.; García-Ruiz, J.; Andrés, N.; Carrasco, R.; Pedraza, J.; Pérez-Alberti, A.; Valcárcel, M.; et al. Late Quaternary glacial phases in the Iberian Peninsula. *Earth Sci. Rev.* **2019**, *192*, 564–600. [[CrossRef](#)]
9. Oliva, M.; Palacios, D.; Fernández-Fernández, J.M. (Eds.) *Iberia, Land of Glaciers: How the Mountains Were Shaped by Glaciers*, 1st ed.; Elsevier: Amsterdam, The Netherlands; Oxford, UK; Cambridge, MA, USA, 2021.
10. Pellitero, R.; Rea, B.R.; Spagnolo, M.; Bakke, J.; Hughes, P.; Ivy-Ochs, S.; Lukas, S.; Ribolini, A. A GIS tool for automatic calculation of glacier equilibrium-line altitudes. *Comput. Geosci.* **2015**, *82*, 55–62. [[CrossRef](#)]
11. Pellitero, R.; Rea, B.R.; Spagnolo, M.; Bakke, J.; Ivy-Ochs, S.; Frew, C.R.; Hughes, P.; Ribolini, A.; Lukas, S.; Renssen, H. GlaRe, a GIS tool to reconstruct the 3D surface of palaeoglaciologists. *Comput. Geosci.* **2016**, *94*, 77–85. [[CrossRef](#)]
12. Oliva, M.; Serrano, E.; Gómez-Ortiz, A.; González-Amuchastegui, M.; Nieuwendam, A.; Palacios, D.; Pérez-Alberti, A.; Pellitero-Ondicol, R.; Ruiz-Fernández, J.; Valcárcel, M.; et al. Spatial and temporal variability of periglacialization of the Iberian Peninsula. *Quat. Sci. Rev.* **2016**, *137*, 176–199. [[CrossRef](#)]
13. Viana-Soto, A.; Pérez-Alberti, A. Periglacial deposits as indicators of paleotemperatures. A case study in the Iberian Peninsula: The mountains of Galicia. *Permafr. Periglac. Process.* **2019**, *30*, 374–388. [[CrossRef](#)]
14. Vieira, G. Combined numerical and geomorphological reconstruction of the Serra da Estrela plateau icefield, Portugal. *Geomorphology* **2008**, *97*, 190–207. [[CrossRef](#)]
15. Palacios, D.; Andrés, N.; de Marcos, J.; Vázquez-Selem, L. Glacial landforms and their paleoclimatic significance in Sierra de Guadarrama, Central Iberian Peninsula. *Geomorphology* **2012**, *139–140*, 67–78. [[CrossRef](#)]
16. Rodríguez-Rodríguez, L.; Jiménez-Sánchez, M.; Domínguez-Cuesta, M.J.; Rinterknecht, V.; Pallàs, R.; Bourlès, D. Chronology of glaciations in the Cantabrian Mountains (NW Iberia) during the Last Glacial Cycle based on in situ-produced ¹⁰Be. *Quat. Sci. Rev.* **2016**, *138*, 31–48. [[CrossRef](#)]
17. Pérez-Alberti, A.; Gómez-Pazo, A. Glaciers Landscapes during the Pleistocene in Trevinca Massif (Northwest Iberian Peninsula). *Land* **2023**, *12*, 530. [[CrossRef](#)]
18. Cowton, T.; Hughes, P.; Gibbard, P. Palaeoglacialization of Parque Natural Lago de Sanabria, northwest Spain. *Geomorphology* **2009**, *108*, 282–291. [[CrossRef](#)]
19. Coudé-Gaussen, G. *Les Serras da Peneda et do Gerês—Étude Geomorphologique*; Centro de Estudos Geográficos: Lisbon, Portugal, 1981; p. 284.
20. Coudé, A.; Coudé-Gaussen, G.; Daveau, S. Nouvelles Observations sur la Glaciation des Montagnes du Nord-Ouest du Portugal. *Cuad. Lab. Xeol. Laxe* **1983**, *5*, 381–393.

21. Figueira, E.; Gomes, A.; Pérez-Alberti, A.; Chaminé, H.I. Moreias da Serra do Soajo: Distribuição e Extensão das Glaciações Plistocénicas. In *O Compromisso da Geografia para Territórios em Mudança: Livro de Atas/XIII Congresso da Geografia Portuguesa*; Associação Portuguesa De Geógrafos: Lisbon, Portugal, 2021; pp. 226–231.
22. Figueira, E.; Gomes, A.; Pérez-Alberti, A.; Chaminé, H.I. 3D modelling of the maximum ice extent and thickness of the palaeoglacier of Serra do Soajo, Northern Portugal. In *Proceedings of the International Congress on Geomorphology*, Coimbra, Portugal, 12–16 September 2022; pp. 2–3. [[CrossRef](#)]
23. Pérez-Alberti, A. The glaciers of the Peneda, Amarela, and Gerês-Xurés massifs. In *Iberia, Land of Glaciers: How the Mountains Were Shaped by Glaciers*; Elsevier: Amsterdam, The Netherlands, 2022; pp. 397–416. [[CrossRef](#)]
24. Carvalho, S.D.E.; Nunes, L. A problemática dos índices glaciários quaternários na Serra do Gêres e na Serra da Peneda (Portugal). *Cad. Lab. Xeolóxico Laxe Rev. Xeol. Galega Hercínico Penins.* **1981**, *2*, 289–298.
25. Ferreira, B. A glaciação Plistocénica da Serra do Gerês. *Finisterra* **1999**, *35*, 39–68.
26. Pereira, P.; Pereira, D.; Casinhas, P. Novos dados sobre a glaciação no sector Gorbelas-Junqueira (Serra da Peneda). *Publicações Assoc. Port. Geomorfólogos* **2009**, *6*, 101–105.
27. Pereira, P.; Pereira, D.I. The Granite and Glacial Landscapes of the Peneda-Gerês National Park. In *Landscapes and Landforms of Portugal*; Springer: Cham, Switzerland, 2020; pp. 127–137. [[CrossRef](#)]
28. João, S.; Lúcio, C.; António, V.; António Bento, G. *Genesis of the Alto Vez Glacial Valley Pleistocene Moraines, Peneda Mountains, Northwest Portugal Caracterização e Génese das Moreias Plistocénicas do Vale Glaciário do Alto Vez, Serra da Peneda, Noroeste de Portugal*; Associação Portuguesa De Geógrafos: Lisbon, Portugal, 2013; pp. 57–62.
29. Santos, J.A.B.; Santos-González, J.; Redondo-Vega, J.M. Till-Fabric analysis and origin of late Quaternary moraines in the Serra da Peneda Mountains, NW Portugal. *Phys. Geogr.* **2015**, *36*, 1–18. [[CrossRef](#)]
30. Martins, C.; Pereira, J.; Pérez-Alberti, A.; Gomes, A. A glaciação Plistocénica do Alto Vez (PNPG): Morfometria dos circos e espessura da língua glaciária. In *A Jangada de Pedra-Geografias Ibero-Afro-Americanas: Atas do Colóquio*; Associação Portuguesa de Geógrafos: Lisbon, Portugal, 2014; pp. 2091–2096.
31. Calicis, E.; Silva, A.; Marques, M.; Martins, C.; Pérez-Alberti, A.; Gomes, A. Recurso a orto-imagens de VANT para a identificação e mapeamento dos testemunhos geomorfológicos da glaciação quaternária nas montanhas do Soajo-Peneda, Portugal. *Assoc. Port. Geomorfólogos Dep. Geogr. FLUP* **2017**, *8*, 6.
32. Osmaston, H. Estimates of glacier equilibrium line altitudes by the Area \times Altitude, the Area \times Altitude Balance Ratio and the Area \times Altitude Balance Index methods and their validation. *Quat. Int.* **2005**, *138–139*, 22–31. [[CrossRef](#)]
33. Ferreira, A.B.; Romani, J.; Zêzere, J.; Rodrigues, M.L. A glaciação pliocénica da serra do Gerês. *Finisterra* **2000**, *69*, 39–68.
34. Daveau, S. Répartition et Rythme des Précipitations au Portugal. *Mem. Cent. Estud. Geográficos* **1977**, *1*, 192.
35. Laboratório Nacional de Energia e Geologia, ‘Geological Charts’. 2020. Available online: https://geoportal.lneg.pt/pt/dados_abertos/cartografia_geologica/cgp50k/ (accessed on 14 March 2020).
36. Lambiel, C.; Maillard, B.; Regamey, B.; Martin, S.; Kummert, M.; Schoeneich, P.; Pellitero, R.P.; Reynard, E. Adaptation of the geomorphological mapping system of the University of Lausanne for ArcGIS. In *Proceedings of the 8th International Conference on Geomorphology of the International Association of Geomorphologists (IAG/AIG)*, Paris, France, 27–31 August 2013; pp. 27–31.
37. James, W.H.; Carrivick, J.L. Automated modelling of spatially-distributed glacier ice thickness and volume. *Comput. Geosci.* **2016**, *92*, 90–103. [[CrossRef](#)]
38. Schilling, D.H.; Hollin, J.T. Numerical Reconstruction of Valley glaciers and small Ice Caps. In *The Last Great Ice Sheets*; Denton, G.H., Hughes, T.J., Eds.; Wiley & Sons: New York, NY, USA, 1981; pp. 207–220.
39. Patterson, W.S.B. The sliding velocity of Athabasca Glacier, Canada. *Polar Cont. Shelf Proj. Dep. Energy Mines Resour. Ott. Ont. Can.* **1970**, *9*, 9. [[CrossRef](#)]
40. Benn, D.; Evans, D.J. *Glaciers & Glaciation*; Hodder Education: London, UK, 1998; Volume 35, p. 6240. [[CrossRef](#)]
41. Braithwaite, R.J.; Muller, F. On the parameterization of glacier equilibrium line altitude. In *Proceedings of the World Glacier Inventory Workshop, Riederalp, Switzerland*, 17–22 September 1978; pp. 263–271.
42. Cogley, L.N.; Hock, J.G.; Rasmussen, L.; Arendt, A.; Bauder, A.; Braithwaite, R.; Jansson, P.; Kaser, G.; Möller, M.; Zemp, M. *Glossary of Glacier Mass Balance and Related Terms*; IHP-VII Te; International Association of Cryospheric Sciences: Paris, France, 2011.
43. Péwé, T.L.; Reger, R.D. Modern and Wisconsinan snowlines in Alaska. *Proc. 24th Int. Geol. Congr. Sect.* **1972**, *12*, 187–197.
44. Benn, D.I.; Lehmkuhl, F. Mass balance and equilibrium-line altitudes of glaciers in high-mountain environments. *Quat. Int.* **2000**, *65–66*, 15–29. [[CrossRef](#)]
45. Egholm, D.L.; Nielsen, S.B.; Pedersen, V.K.; Lesemann, J.E. Glacial effects limiting mountain height. *Nature* **2009**, *460*, 884–887. [[CrossRef](#)]
46. Lichtenecker, V. *Die Gegenwärtige und die Eiszeitliche Schneegrenze in den Ostalpen*; no. Verhandlungsband der III; Vienna, Austria, *Quaternary Conference*; 1938; Volume III, pp. 141–147.
47. Kerschner, H.; Kaser, G.; Sailer, R. Alpine Younger Dryas glaciers as palaeo-precipitation gauges. *Ann. Glaciol. Int. Glaciol. Soc.* **2000**, *31*, 80–84. [[CrossRef](#)]
48. Porter, S.C. Snowline depression in the tropics during the Last Glaciation. *Quat. Sci. Rev.* **2000**, *20*, 1067–1091. [[CrossRef](#)]

49. Benn, D.I.; Ballantyne, C.K. Palaeoclimatic reconstruction from Loch Lomond Readvance glaciers in the West Drumochter Hills, Scotland. *J. Quat. Sci.* **2005**, *20*, 577–592. [[CrossRef](#)]
50. Benn, D.I.; Hulton, N.R. An Excel™ spreadsheet program for reconstructing the surface profile of former mountain glaciers and ice caps. *Comput. Geosci.* **2010**, *36*, 605–610. [[CrossRef](#)]
51. Rea, B.R. Defining modern day Area-Altitude Balance Ratios (AABRs) and their use in glacier-climate reconstructions. *Quat. Sci. Rev.* **2009**, *28*, 237–248. [[CrossRef](#)]
52. Bahr, D.B. Estimation of Glacier Volume and Volume Change by Scaling Methods. *Earth Sci. Ser.* **2012**, *3*, 278–280. [[CrossRef](#)]
53. Pérez-Alberti, A.; Guitián, M.R.; Valcárcel, M. *Las Formas y Depósitos Glaciares en las Sierras Orientales y Septentrionales de Galicia (NW Península Ibérica)*; Universidade de Santiago de Compostela: Santiago, Spain, 1993.
54. Daveau, S.; Devy-Vareta, N. Gelifraction, nivation et glaciation d’abri de la Serra da Cabreira. *Actas* **1985**, *1*, 75–84.
55. Pérez-Alberti, A.; Valcarcel, M. The glaciers in Eastern Galicia. In *Iberia, Land of Glaciers: How the Mountains Were Shaped by Glaciers*; Elsevier: Amsterdam, The Netherlands, 2022; pp. 375–395. [[CrossRef](#)]
56. Valcarcel, M.; Pérez-Alberti, A. The glaciers in Western Galicia. In *Iberia, Land of Glaciers: How the Mountains Were Shaped by Glaciers*; Elsevier: Amsterdam, The Netherlands, 2022; pp. 353–373. [[CrossRef](#)]
57. Vizmidt-Thomé, M. New, low-lying witnesses of a Würmian glaciation in the northern part of the Iberian Peninsula (Prov. Vizcaya and Orense, Spain and Minho district, Portugal). In *Late-and Postglacial Oscillations of Glaciers: Glacial and Periglacial Form*; CRC Press, Schweizerbart: Stuttgart, Germany, 1983; Volume. 23/24, pp. 384–389.
58. De Luis, M.; Brunetti, M.; Gonzalez-Hidalgo, J.C.; Longares, L.A.; Martin-Vide, J. Changes in seasonal precipitation in the Iberian Peninsula during 1946–2005. *Glob. Planet. Chang.* **2010**, *74*, 27–33. [[CrossRef](#)]
59. Cortesi, N.; Gonzalez-Hidalgo, J.C.; Trigo, R.M.; Ramos, A.M. Weather types and spatial variability of precipitation in the Iberian Peninsula. *Int. J. Climatol.* **2014**, *34*, 2661–2677. [[CrossRef](#)]
60. Peña-Angulo, D.; Trigo, R.; Cortesi, N.; González-Hidalgo, J. The influence of weather types on the monthly average maximum and minimum temperatures in the Iberian Peninsula. *Atmos. Res.* **2016**, *178–179*, 217–230. [[CrossRef](#)]
61. Pereira, P.; Binnie, S.; Dunai, T.; Henriques, R.; Pereira, D. On the age and extent of the Serra da Peneda glaciation, NW Portugal. *Int. Congr. Geomorphol.* **2022**, *1*. [[CrossRef](#)]
62. Pérez-Alberti, A.; Díaz, M.V.; Martini, I.P.; Pascucci, V.; Andreucci, S. Upper Pleistocene glacial valley-junction sediments at Pias, Trevinca Mountains, NW Spain. *Geol. Soc. Lond. Spéc. Publ.* **2011**, *354*, 93–110. [[CrossRef](#)]
63. Pérez-Alberti, A.; Díaz, M.V.; Chao, R.B. Pleistocene glaciation in Spain. In *Developments in Quaternary Sciences*; Elsevier: Amsterdam, The Netherlands, 2004; pp. 389–394. [[CrossRef](#)]
64. Rodríguez-Rodríguez, L.; Jiménez-Sánchez, M.; Domínguez-Cuesta, M.J.; Rinterknecht, V.; Pallàs, R.; Bourlès, D.; Valero-Garcés, B. A multiple dating-method approach applied to the Sanabria Lake moraine complex (NW Iberian Peninsula, SW Europe). *Quat. Sci. Rev.* **2014**, *83*, 1–10. [[CrossRef](#)]
65. Vidal Romaní, J.R.; Mosquera, D.F. Glaciarismo Pleistoceno en el NW de la Península Ibérica (Galicia, España-Norte de Portugal), Enseñ. Las Cienc. Tierra, no. January. 2005. Available online: <https://dialnet.unirioja.es/servlet/articulo?codigo=2898676> (accessed on 25 February 2020).
66. Ballantyne, C.K. A general model of paraglacial landscape response. *Holocene* **2002**, *12*, 371–376. [[CrossRef](#)]
67. Cossart, E.; Braucher, R.; Fort, M.; Bourlès, D.; Carcaillet, J. Slope instability in relation to glacial debuttressing in alpine areas (Upper Durance catchment, southeastern France): Evidence from field data and ¹⁰Be cosmic ray exposure ages. *Geomorphology* **2008**, *95*, 3–26. [[CrossRef](#)]
68. Carrasco, R.M.; Pedraza, J.; Palacios, D. The glaciers of the Sierra de Gredos. In *Iberia, Land of Glaciers: How the Mountains Were Shaped by Glaciers*; Elsevier: Amsterdam, The Netherlands, 2022; pp. 457–483. [[CrossRef](#)]
69. Gil García, M.; Valiño, M.D.; Rodríguez, A.V.; Zapata, M.R. Late-glacial and Holocene palaeoclimatic record from Sierra de Cebollera (northern Iberian Range, Spain). *Quat. Int.* **2002**, *93–94*, 13–18. [[CrossRef](#)]
70. Ballantyne, C.K. After the Ice: Holocene Geomorphic Activity in the Scottish Highlands. *Scott. Geogr. J.* **2008**, *124*, 8–52. [[CrossRef](#)]

Disclaimer/Publisher’s Note: The statements, opinions and data contained in all publications are solely those of the individual author(s) and contributor(s) and not of MDPI and/or the editor(s). MDPI and/or the editor(s) disclaim responsibility for any injury to people or property resulting from any ideas, methods, instructions or products referred to in the content.